SCIENTIFIC REPORTS

OPEN

SUBJECT AREAS:
PALAEOCLIMATE
GEOLOGY

Received
5 June 2014

Accepted
28 August 2014

Published
22 October 2014

Correspondence and requests for materials should be addressed to X.L. (xingqiliu@yahoo.com; xqliu@niglas.ac.cn)

A less or more dusty future in the Northern Qinghai-Tibetan Plateau?

Xingqi Liu[1,2], Zhitong Yu[3,4,5], Hailiang Dong[6,7] & Huei-Fen Chen[8]

[1]College of Environmental Resources & Tourism, Capital Normal University, Beijing, P.R. China, [2]State Key Laboratory of Lake Science and Environment, Nanjing Institute of Geography and Limnology, Chinese Academy of Sciences, Nanjing, P.R. China, [3]State Key Laboratory of Desert and Oasis Ecology, Xinjiang Institute of Ecology and Geography, Chinese Academy of Sciences, Urumqi, Xinjiang, P.R. China, [4]University of Chinese Academy of Sciences, Beijing, P.R. China, [5]College of Resources and Environmental Sciences, Xinjiang University, Urumqi, China, [6]State Key Laboratory of Biogeology and Environmental Geology, China University of Geosciences, Beijing, P.R. China, [7]Department of Geology and Environmental Earth Science, Miami University, Oxford, OH45056, USA, [8]Institute of Applied Geosciences, National Taiwan Ocean University, Taiwan, R.O.C.

Dust plays an important role in climate changes as it can alter atmospheric circulation, and global biogeochemical and hydrologic cycling. Many studies have investigated the relationship between dust and temperature in an attempt to predict whether global warming in coming decades to centuries can result in a less or more dusty future. However, dust and temperature changes have rarely been simultaneously reconstructed in the same record. Here we present a 1600-yr-long quantitative record of temperature and dust activity inferred simultaneously from varved Kusai Lake sediments in the northern Qinghai–Tibetan Plateau, NW China. At decadal time scale, our temperature reconstructions are generally in agreement with tree-ring records from Karakorum of Pakistan, and temperature reconstructions of China and North Hemisphere based on compilations of proxy records. A less or more dusty future depends on temperature variations in the Northern Qinghai-Tibetan Plateau, i.e. weak and strong dust activities at centennial time scales are well correlated with low and high June–July–August temperature (average JJA temperature), respectively. This correlation means that stronger summer and winter monsoon should occur at the same times in the northern Qinghai–Tibetan Plateau.

The Qinghai–Tibetan Plateau (QTP) plays an important role in the evolution of Asian monsoon and is particularly sensitive to global climate change[1]. Over the past thirty years, paleoclimatologists have reconstructed many records at millennial time scales from lake sediments in the QTP[2–5]. Studies on ice cores[6–8], tree rings[9,10], and lake sediments[11] also provided some information about the decadal to centennial scale climate variability in the QTP. However, high-resolution climate records are still limited for the QTP. In particular, quantitative climate records are sparse. Lack of this information has greatly hindered our understanding of the QTP climate variability at the decadal to centennial time scales.

Kusai Lake (35°37′–35°50′ N, 92°38′–93°15′ E, 4475 m a.s.l.), a saline lake with a present-day salinity of 28.54 g/l, is situated in the largest almost uninhabited Hoh Xil region of the Northern Qinghai-Tibetan Plateau, NW China (Fig. 1). The 53-year (1957–2009) meteorological data from the Wudaoliang Station (35.22° N, 93.08° E, about 50 km southwest of Kusai Lake) indicate a mean annual temperature of about −5.4°C, a mean annual precipitation of 283 mm, and a mean annual wind speed of about 4.4 m/s. Mean monthly precipitation is higher between May and September than in other months (Supplementary Fig. S1A). Warm temperatures (above 0°C) occur from June to September (Supplementary Fig. S1A). Mean monthly wind speed is higher in winter than in other seasons (Supplementary Fig. S1B).

Results

The Kusai lake sediment cores are well rhythmically laminated. In thin section, the couplets are made of dark reddish-brown silt-sand capped by lighter silt-clay (Supplementary Fig. S2A). Couplets are present throughout the core, indicating continuous rhythmic deposition. The dark units are generally thin with an average thickness of 0.58 mm (Supplementary Fig. S3A), and are composed of quartz and feldspar. In some cases, the dark layers form discrete, unsorted grains with 2 mm or more in diameter and the thickness can reach 1 to 2 cm (Supplementary Fig. S2B). The physical features (e.g., grain size and color) of the dark layers are quite similar to those of aeolian deposits that we collected across lake ice in winter. The light layers are thicker than the dark layers with an average thickness of 1.62 mm (Supplementary Fig. S3B), mainly composed of clay minerals and

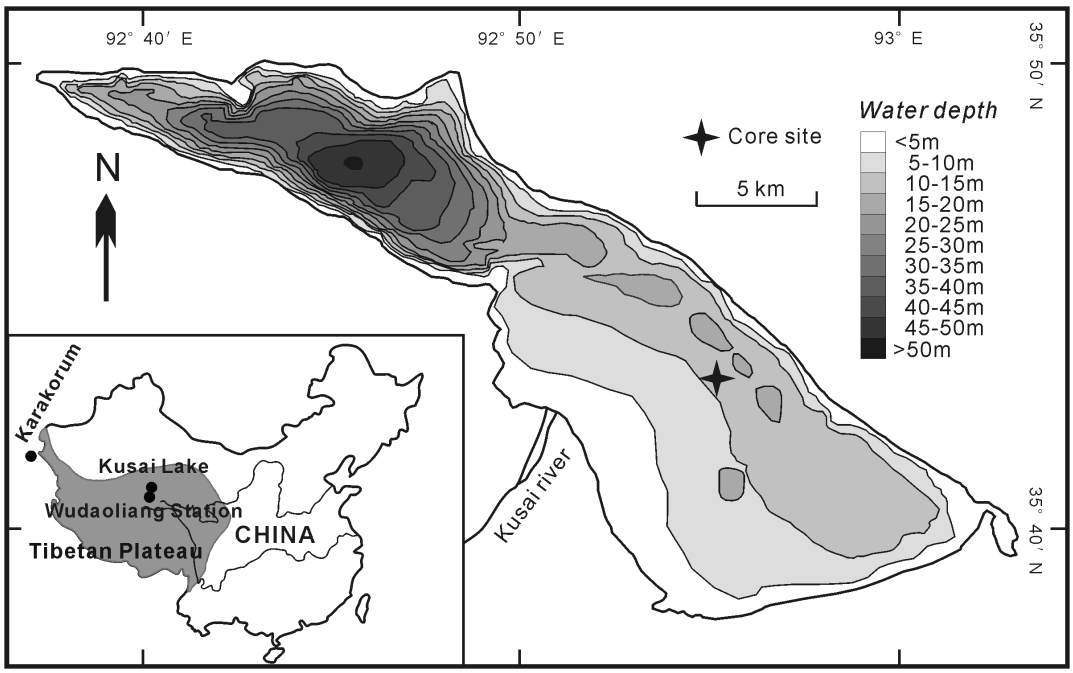

Figure 1 | **Location of Kusai Lake and the coring site.** Also shown are the locations of Wudaoliang station and Karakorum. Bathymetric was measured in 2002 and bathymetric contours were plotted by using software surfer 10.

carbonates, and contain many ostracod shells and Cladocera remains. The mineral compositions of single dark and light layers are quite different. Light layers contain ca 13–20% aragonite which is an authigene mineral while dark layers do not contain aragonite (Supplementary Table S1). Accordingly, we suggest that dark layers are formed by coarse sand and silt that were deposited on lake ice by aeolian processes during winter. Upon ice thawing during summer, these sands and silts may be released and deposited into lake sediments. The light layers are interpreted to represent summer season accumulations, when carbonates deposited, and Ostracodes and Cladocera grew under warm temperature conditions.

Previous studies have demonstrated that varve-thickness records from glacial-fed lakes are physically linked temperatures and should provide a record of past summer temperatures[12,13]. Warm summers can often result in significant melting of glaciers and snowmelt, and thus lead to high runoff and sediment flux to lakes[12,13]. As light layers of varved Kusai Lake sediments are formed during summers, we compare thicknesses of light layers (LT) with summer temperatures (June–July–August, average JJA temperatures) from the Wudaoliang station (Supplementary Fig. S4), the nearest available meteorological data. Average JJA temperatures and thicknesses of light layers between 1957 and 2009 AD show a positive relationship (Supplementary Fig. S4C, $r = 0.534$, $p = 0.01$, $n = 53$): $T_{JJA} = 0.51 \times LT + 3.93$, where T_{JJA} is the average summer temperature (°C), and LT is the thickness of light layers (mm).

Based on the above formula, we estimate JJA temperature from 350 to 2010 AD (Fig. 2A). In order to reveal a long-term temperature record, a 51-year moving average was obtained to smooth temperature variations. According to the JJA temperature variation (Fig. 2A), there is a cooling period from 350 to 600 AD, which corresponds to the Dark Age Cold Period (DACP). This cooling period is consistent with China temperature variations based on compilations of proxy records[14] (Fig. 2D). Following this cooling period, temperatures increased until 1250 AD. There are two warm periods from 600 to 720 AD and from 800 to 1100 AD (Fig. 2A), which are well correlated with the Sui and Tang dynasty warm period in China and the Medieval Warm Period in Europe, respectively. The latter is the warmest period in Kusai Lake for the last 1600 years (Fig. 2A). This period is characterized by two temperature peaks around 900 and 1000 AD. A 1300 year climatic record from tree-rings of the Karakorum in Pakistan also shows that the warmest conditions occurred between 800 and 1100 AD[15] (Fig. 2C). Beginning at 1250 AD, the temperature decreased until 1760 AD and the northern Qinghai–Tibetan Plateau experienced a cold period of the so-called Little Ice Age (LIA) (Fig. 2A). This cold period is also recorded in many regions of China[14]. After the LIA stage, temperature began to increase (Fig. 2A).

Our reconstructed temperature records based on varve thickness from Kusai Lake show a positive correlation with tree-ring records from Karakorum of Pakistan at annual time scale[15] (Fig. 2C, $r = 0.115$, $p = 0.01$, $n = 1356$), and with temperature reconstructions of China (Fig. 2.C, $r = 0.256$, $p = 0.01$, $n = 162$) and the North Hemisphere (Fig. 2.D, $r = 0.242$, $p = 0.01$, $n = 162$) based on compilations of proxy records at decadal time scale[14,16]. So, our reconstructed temperature records are generally in agreement with tree-ring records Karakorum of Pakistan at annual time scale, and temperature reconstructions of China and the North Hemisphere based on compilations of proxy records at decadal time scale. However, the amplitude of temperature decrease during the LIA stage in the northern Qinghai–Tibetan Plateau is lower than that of reconstructed temperatures in China and the North Hemisphere[14,16] (Fig. 2A, 2C, and 2D). The amplitude of temperature decrease based on the tree-ring records Karakorum[15] during the LIA stage is also small (Fig. 2B). This is probably because the accumulation of light layers of varved kusai Lake sediments and the growth of tree ring mainly occur in summer season, which possibly indicates that the cooling of summer temperature is to a lesser extent than that of winter temperature during the LIA stage. Another difference is that there is no trend in temperature in the Kusai Lake record over the 20th century (Fig. 2A). The reason for this is possibly due to that the 20th century warming is not obvious in the Northern Qinghai-Tibetan Plateau. Karakorum tree ring records also show that there is no obvious 20th century warming (Fig. 2.B).

Kusai Lake is located in the Hoh Xil region which experiences the highest frequency of dust storms in Qinghai Province[17]. The meteorological data from the Wudaoliang station shows that wind speed

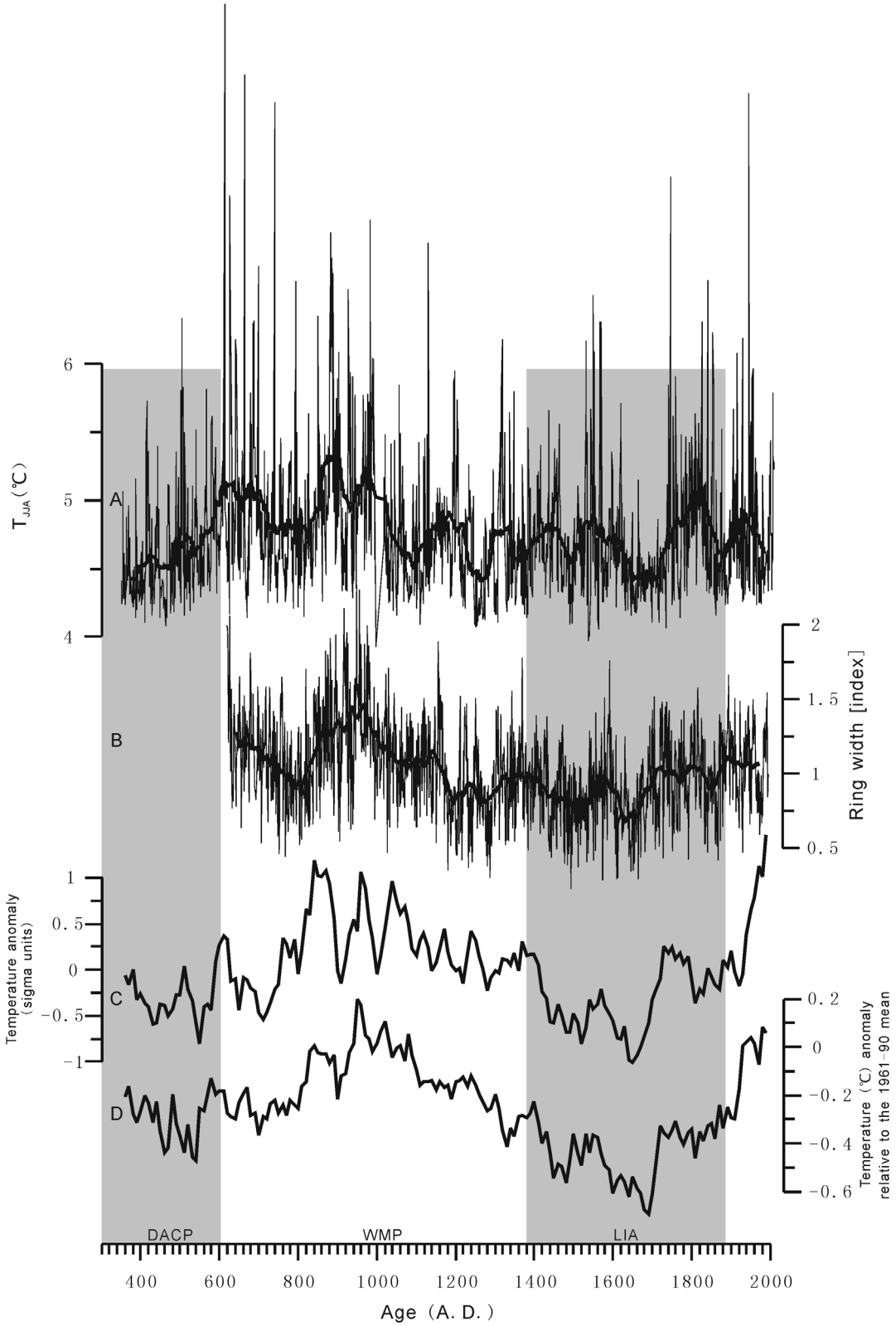

Figure 2 | T_{JJA} reconstructions from varved Kusai Lake during the last 1600 years (A), and their comparisons with tree-ring records from Karakorum in Pakistan(B)[15], and temperature reconstructions of China (C)[14], and North Hemisphere (D)[16]. DACP, MWP, LIA, and CWP refer to Dark Age Cold Period, Medieval Warm Period, Little Ice Age, respectively.

is generally high in winter (Supplementary Fig. S1B). The strong winter wind can result in dust storm and aeolian sediment flux to lake ice. Therefore, we compare the thicknesses of dark layers (DT) with average wind speed (AWS) from the Wudaoliang station (Supplementary Fig. S5A and B). The result shows that DT is positively correlated with AWS from 1957 to 2009 AD: AWS = 6.28 ×

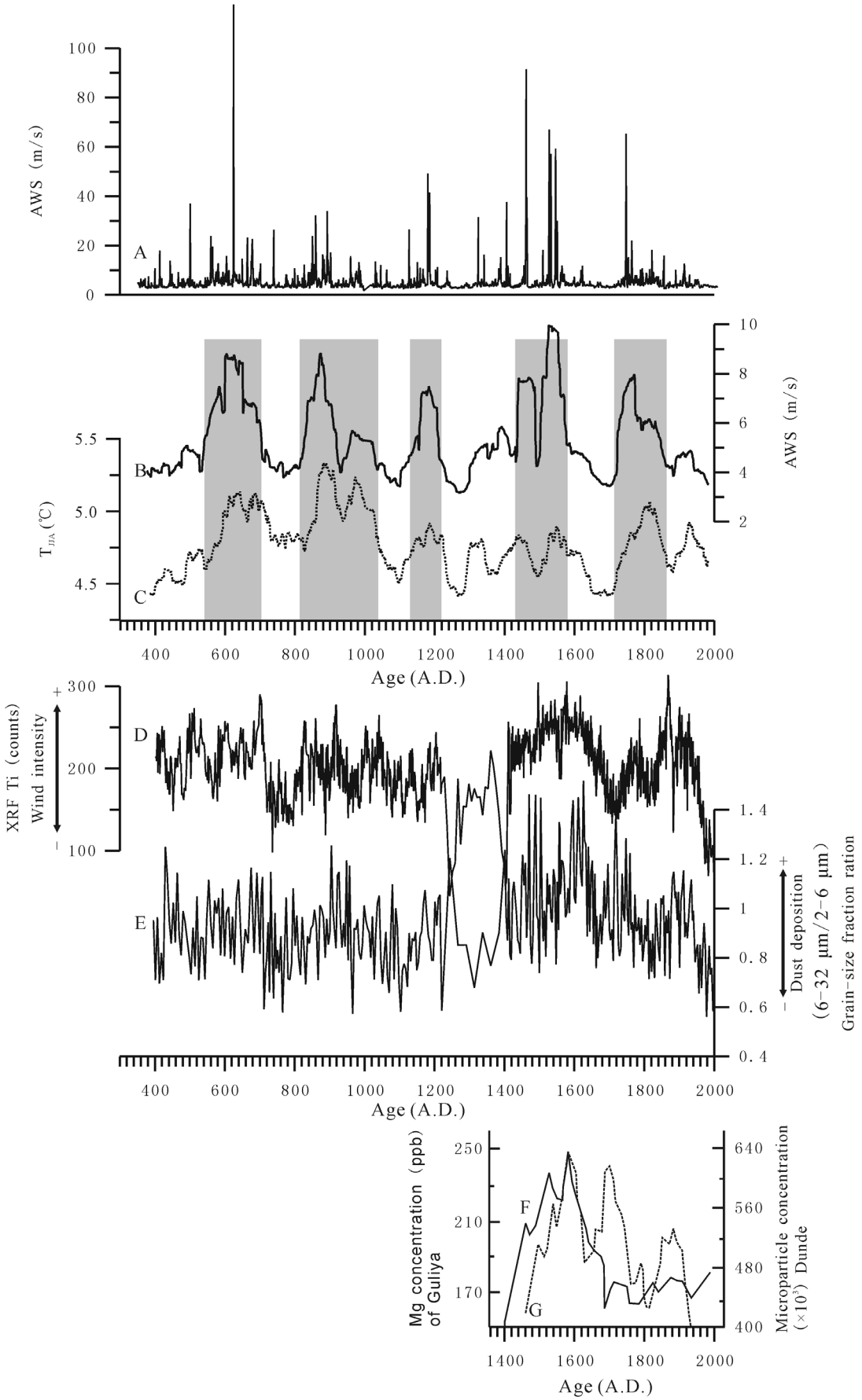

Figure 3 | Reconstruction of average wind speed (AWS) (A, B), and its comparison with T_{JJA} in Kusai Lake (C), Ti content (D)[20] and the grain-size fraction ratio between 6–32 μm and 2–6 μm from sediment core of the Aral Sea (E)[21], and the Mg^{2+} concentration from the Guliya ice core (F) and the microparticle concentration of the Dunde ice core (G)[8]. (B) and (C) are 51-year moving average of AWS and T_{JJA}, respectively.

DT + 1.70 (Supplementary Fig. S5C, r = 0.733, p = 0.01, n = 53), where AWS is the average of annul wind speed (m/s), and DT is the thickness of the dark layer (mm).

Based on the above formula, we calculate the AWS from 350 to 2010 AD (Fig. 3A). In order to highlight long-term AWS variations, a 51-year moving average was obtained to smooth AWS reconstruction (Fig. 3B). Five high AWS periods, 520–700 AD, 820–1040 AD, 1130–1220 AD, 1430–1580 AD, and 1720–1860 AD, are revealed, which suggests that dust activity is strong during these five periods (Fig. 3A and B). Between these five high AWS periods, there are six low AWS periods occurring in 350–520 AD, 700–820 AD, 1040–1130 AD, 1220–1430 AD, 1580–1720 AD, 1860- present, suggesting a week dust activity (Fig. 3A and B). The variations of dust activity in Kusai Lake record are generally in agreement with those inferred from Ti content (Fig. 3D)[18] and the ratio of the grain-size fraction of 6–32 μm over 2–6 μm from sediment core of the Aral Sea over the last 2000 years (Fig. 3E)[19]. The highest dust activity in our record occurred in 1430–1580 AD, which corresponds to the LIA. Dust records indicated by the Mg^{2+} concentration from the Guliya ice core (Fig. 3F) and the microparticle concentration of the Dunde ice core (Fig. 3G) during the last 600 years also show that the strongest intensity of dust storms occurred from 1450 to 1650 AD[8]. This phenomenon had also been recorded in Juyanhai lake, where a most terrible dust storm caused desertification during 1550 AD in northwest China[20].

Discussion

At large time scale (such as glacial to interglacial transitions), records from loess sediments, and ice cores indicate that dust concentrations were higher in glacial periods than in interglacial periods[21,22]. Similarly, regional characteristics of dust storms from 135 stations in northern China from 1954 to 1998 indicate that there is a negative correlation between prior winter temperature and dust storm frequency for most stations[23]. Simulations on atmospheric dust loading also suggest that future dust may be 20 to 60% lower than current dust loadings if the global temperature continues to rise[24]. These results suggest that high atmospheric dusting loading results from temperature increase. In contrast, three-dimensional climate simulations suggest that high glacial dust loading may have caused significant, episodic regional warming of over 5°C downwind of major Asian and ice-margin dust sources[25]. In contrast to the negative correlation between dust activity and temperature at glacial - interglacial time scale (tens of thousands of years), at decadal to centennial time scales, dust records from Dasuopu and East Rongbuk ice core in the Tibetan Plateau show a significant positive relationship between the dust concentration and reconstructed air temperatures during the last 600 years[26–28]. Conroy et al. (2010) reached the same conclusion based on studies of sediment records from two lakes, Kiang Co and Ngamring Co, in southwestern Tibet over the last ~100 years[29]. Similarly, in the southern Hemisphere, ice core record of aluminum deposition in the northern Antarctic Peninsula shows that aluminosilicate dust deposition was more than doubled during the 20th century relative to previous centuries, and this increased dust deposition was coincident with the 1°C Southern Hemisphere warming[30].

The inconsistency between dust activity and temperature (either negative or positive) is partly caused by different records used for dust activity and temperature reconstructions. In this case, different age models and inter-record correlations can all introduce errors. In our study, both dust activity and temperature are reconstructed from the same record which should have eliminated these errors. There is a weak positive relationship between the light and dark laminae thickness (r = 0.169, p = 0.01, n = 1639) at annual time scale, but the correlation coefficient increases highly after a 51-year moving average was made (r = 0.57, p = 0.01, n = 1589), which indicates that week and strong dust activities at centennial time scales are well correlated with low and high JJA temperatures (Fig. 3B and C), respectively. Accordingly, a less or more dusty future depends on temperature variations in the Northern Qinghai-Tibetan Plateau. Ruddiman indicated that more intense summer insolation maxima and deeper winter insolation minima always occur together at any one location[31]. As a result, stronger summer monsoon should occur at the same times in the past with stronger winter monsoon. The positive relationship between the light and dark laminae thickness suggests that increased temperatures led to strong dust activity, while decreased temperatures resulted in weak dust activity in the northern Qinghai–Tibetan Plateau. Our records show that, at annual time scales, especially at centennial time scales, stronger summer and winter monsoon should occur at the same times.

Methods

In september 2006, a 3.5 m long sediment core was recovered from the southeastern region of Kusai Lake at a water depth of 14.5 m using UWITEC coring equipment, and two short cores (29 cm and 43 cm in length, respectively) parallel to the long core were collected using a gravity corer (Fig. 1). The long sediment core (3.5 m in length) and a short core (43 cm in length) were used for thin section preparation. Undisturbed sediment slabs (7 × 1.5 × 1 cm) were collected continuously down core with 2 cm of overlap between two consecutive slabs to ensure that all couplets of varves were represented. All sediment slabs were freeze-dried and embedded with low viscosity epoxy resin under low vacuum. Following impregnation, sediment slabs were cut length-wise, and ground to a thickness of approximately 40 μm (Supplementary Fig. S6). Optical microscope analyses were performed to study sedimentary microfacies, to count varves, and to measure the varve thickness.

The 29 cm short core was sampled at 0.5 cm intervals in the laboratory and core slices were radiometrically dated by measuring ^{210}Pb and ^{137}Cs activity as a function of depth. Sedimentation rates and chronologies were calculated using the ^{210}Pb data and the constant initial concentration model (CIC), which assumes that the sediments have a constant initial excess lead-210 concentration[32]. ^{137}Cs activity was measured to check the ^{210}Pb-derived dates. AMS ^{14}C ages from seventeen levels in the long core were determined on bulk organic carbon at Rafter Radiocarbon Laboratory, Institute of Geological and Nuclear Sciences (GNS), New Zealand, and Beta Analytic Inc. (Miami, Florida, USA), and AMS Lab of Peking University, China (Supplementary Table S2).

Varves were counted at least three times to ensure data quality and consistency. We estimate an approximate 1% error in varve ages based on replicate counts. The initial rise in the ^{137}Cs activity occurs at 11.0 cm and can probably be ascribed to the onset of significant fallout in 1954 AD in the northern hemisphere (Supplementary Fig. S7A). A ^{137}Cs peak at 8.5 cm corresponds to 1963 AD (Supplementary Fig. S7A). The ^{210}Pb-based chronology (CIC model) is generally in good agreement with the ^{137}Cs-based chronology (Supplementary Fig. S7A). In addition, ages determined from couplet counting fit well with the ^{210}Pb and ^{137}Cs ages (Supplementary Fig. S7A).

The age (^{14}C)/depth correlation for the Kusai Lake record is shown in Supplementary Fig. S7. A comparison of the ^{210}Pb- and ^{137}Cs-based ages (1950 AD or 0 yr BP) with the linearly fitted ^{14}C age at the same depth (11-cm) (i.e., 3180 yr BP) suggests that the radiocarbon age is in excess of the ^{210}Pb and ^{137}Cs age by 3180 yrs (Supplementary Fig. S7B) which is similar to our previous results[11,33]. A reservoir effect caused by dating of aquatic plants or lacustrine algae could account for this time excess by ^{14}C dating. In these aquatic plants and lacustrine algae, carbon could be directly derived from hard-water lakes, which is a common problem in the radiocarbon dating of lacustine sediments in the arid-semiarid regions of Western China[34]. Thus, we subtracted 3180 years from all ^{14}C ages prior to calibration. The calibration and age-depth model were constructed using the recently developed Bayesian method[35], which takes the accumulation rates into account. The model was carried out using the default settings for lake sediments with 5-cm resolution, and calibrated using the IntCal09 dataset[36] (Supplementary Fig. S7B). Age difference between varve age and calibrated age still exists, which varies from 9 to 457 years. This indicates that the ^{14}C reservoir effect correction of 3180 yr was not constant due to negative or positive hydrologic budget in Kusai Lake over the past 1600 yr. In spite of this, many calibrated ages still agree well with those from couplet counting. Thus, ^{137}Cs, ^{210}Pb, ^{14}C, and varve counting results suggest that the sediment couplets in Kusai Lake sediments are varves (Supplementary Fig. S7A and 7B). Our age model is based on varve counting.

1. An, Z., John, E. K., Warren, L. P. & Stephen, C. P. Evolution of Asian monsoons and phased uplift of the Himalaya-Tibetan plateau since Late Miocene times. *Nature* **411**, 62–66 (2001).
2. Lister, G. S., Kelts, K., Chen, K., Yu, J. & Niessen, F. Lake Qinghai, China: closed-basin lake levels and the oxygen isotope record for ostracoda since the latest Pleistocene. *Paleogeogr. Paleoclimatol. Paleoecol.* **84**, 141–162 (1991).
3. Gasse, F. *et al.* A 13000-year climate record from western Tibet. *Nature* **353**, 742–745 (1991).
4. Shen, J., Liu, X., Wang, S. & Matsumoto, R. Palaeoclimatic changes in the Qinghai Lake area during the last 18,000 years. *Quat. Int.* **136**, 131–140 (2005).

5. Herzschuh, U., Winter, K., Wünnemann, B. & Li, S. A general cooling trend on the central Tibetan Plateau throughout the Holocene recorded by the Lake Zigetang pollen spectra. *Quat. Int.* **154–155**, 113–121 (2006).
6. Thompson, L. G. *et al*. Holocene-Late Pleistocene Climatic Ice Core Records from Qinghai-Tibetan Plateau. *Science* **246**, 474–477 (1989).
7. Yao, T. & Thompson, L. G. Trends and features of climatic changes in the past 5000 years recorded by the Dunde ice core. *Ann. Glaciol.* **16**, 21–24 (1992).
8. Yang, M., Yao, T. & Wang, H. Microparticle content records of the Dunde ice core and dust storms in northwestern China. *J. Asian Earth Sci.* **27**, 223–229 (2006).
9. Shao, X. *et al*. Reconstruction of precipitation variation from tree rings in recent 1000 years in Delingha, Qinghai. *Sci. China Ser. D-Earth Sci.* **48**, 939–949 (2005).
10. Zhang, Q., Cheng, G., Yao, T., Kang, X. & Huang, J. A 2,326 year tree-ring record of climate variability on the northeastern Qinghai-Tibetan Plateau. *Geophys. Res. Lett.* **30**, 1739–1741 (2003).
11. Liu, X. *et al*. Late Holocene forcing of the Asian winter and summer monsoon as evidenced by proxy records from the northern Qinghai-Tibetan Plateau. *Earth Planet. Sci. Lett.* **280**, 276–284 (2009).
12. Moore, J. J., Hughen, K. A., Miller, G. H. & Overpeck, J. T. Little Ice Age recorded in summer temperature reconstruction from vared sediments of Donard Lake, Baffin Island, Canada. *J. Paleolimnol.* **25**, 503–517 (2001).
13. Loso, M. G., Anderson, R. S., Anderson, S. P. & Reimer, P. J. A 1500-year record of temperature and glacial response inferred from varved Iceberg Lake, southcentral Alaska. *Quat. Res.* **66**, 12–24 (2006).
14. Yang, B., Braeuning, A., Johnson, K. R. & Yafeng, S. General characteristics of temperature variation in China during the last two millennia. *Geophys. Res. Lett.* **29**, 381–384 (2002).
15. Esper, J., Schweingruber, F. H. & Winiger, M. 1300 years of climatic history for Western Central Asia inferred from tree-rings. *Holocene* **12**, 267–277 (2002).
16. Ljungqvist, F. C. A new reconstruction of temperature variability in the extra-tropical Northern Hemisphere during the last two millennia. *Geogr. Ann. Ser. A-Phys. Geogr.* **92**, 339–351 (2010).
17. Fang, Z. Y., Zhu, F. K., Jiang, J. X. & Qian, Z. A. *Research of Dust-storm in China*. (Meteorological Press, 1997).
18. Sorrel, P. *et al*. Control of wind strength and frequency in the Aral Sea basin during the late Holocene. *Quat. Res.* **67**, 371–382 (2007).
19. Huang, X., Oberhänsli, H., Von Suchodoletz, H. & Sorrel, P. Dust deposition in the Aral Sea: implications for changes in atmospheric circulation in central Asia during the past 2000 years. *Quat. Sci. Rev.* **30**, 3661–3674 (2011).
20. Chen, H.-F. *et al*. A multiproxy lake record from Inner Mongolia displays a late Holocene teleconnection between Central Asian and North Atlantic climates. *Quat. Int.* **227**, 170–182 (2010).
21. Jouzel, J. *et al*. Extending the Vostok ice-core record of palaeoclimate to the penultimate glacial period. *Nature* **364**, 407–412 (1993).
22. Wolff, E. W. *et al*. Southern Ocean sea-ice extent, productivity and iron flux over the past eight glacial cycles. *Nature* **440**, 491–496 (2006).
23. Qian, W., Tang, X. & Quan, L. Regional characteristics of dust storms in China. *Atmos. Environ.* **38**, 4895–4907 (2004).
24. Mahowald, N. M. & Luo, C. A less dusty future? *Geophys. Res. Lett.* **30**, 1903, doi:10.1029/2003GL017880 (2003).
25. Overpeck, J., Rind, D., Lacis, A. & Healy, R. Possible role of dust-induced regional warming in abrupt climate change during the last glacial period. *Nature* **384**, 447–449 (1996).
26. Xu, J. *et al*. A 108.83-m ice-core record of atmospheric dust deposition at Mt. Qomolangma (Everest), Central Himalaya. *Quat. Res.* **73**, 33–38 (2010).
27. Thompson, L. G. *et al*. A high-resolution millennial record of the South Asian monsoon from Himalayan ice cores. *Science* **289**, 1916–1919 (2000).
28. Conroy, J. L. *et al*. Dust and temperature influences on glaciofluvial sediment depositionin southwestern Tibet during the last millennium. *Global Planet. Change* **107**, 132–144 (2013).
29. Conroy, J. L., Overpeck, J. T., Liu, K. & Wang, L. in *AGU Fall Meeting Abstracts*. 07.
30. McConnell, J. R., Aristarain, A. J., Banta, J. R., Edwards, P. R. & Simões, J. C. 20th-Century doubling in dust archived in an Antarctic Peninsula ice core parallels climate change and desertification in South America. *Proc. Natl. Acad. Sci. U. S. A.* **104**, 5743–5748 (2007).
31. Ruddiman, W. F. *Earth's Climate: Past and Future*. (WH freeman and company, 2008).
32. Appleby, P. G. & Oldfield, F. The calculation of ^{210}Pb dates assuming a constant rate of supply of unsupported ^{210}Pb to the sediment. *Catena* **5**, 1–8 (1978).
33. Wu, X. *et al*. Evaluation of glycerol dialkyl glycerol tetraether proxies for reconstruction of the paleo-environment on the Qinghai-Tibetan Plateau. *Org. Geochem.* **61**, 45–56 (2013).
34. Hou, J., D'Andrea, W. J. & Liu, Z. The influence of ^{14}C reservoir age on interpretation of paleolimnological records from the Tibetan Plateau. *Quat. Sci. Rev.* **48**, 67–79 (2012).
35. Blaauw, M. & Christen, J. A. Flexible paleoclimate age-depth models using an autoregressive gamma process. *Bayesian Analysis* **6**, 457–474 (2011).
36. Reimer, P. J. *et al*. IntCal09 and Marine09 radiocarbon age calibration curves, 0–50,000 years cal BP. *Radiocarbon* **51**, 1111–1150 (2009).

Acknowledgments

We thank Wang Jianjun and Yang Bo for their help with fieldwork. This work was supported by the CAS Strategic Priority Research Program (Grant No. XDA05080403), China Global Change Research Program (Grant No. 2012CB956101), the National Natural Science Foundation of China (NSFC Grant No. 41030211), and State Key Laboratory of Lake Science and Environment (2014SKL001).

Author contributions

X.L. conceived and designed the experiments. Z.Y. performed the experiments. X.L., H.D. and C.H. co-wrote the paper. All authors discussed the results.

Additional information

Supplementary information accompanies this paper at http://www.nature.com/scientificreports

Competing financial interests: The authors declare no competing financial interests.

How to cite this article: Liu, X., Yu, Z., Dong, H. & Chen, H.-F. A less or more dusty future in the Northern Qinghai-Tibetan Plateau? *Sci. Rep.* **4**, 6672; DOI:10.1038/srep06672 (2014).